

This document is confidential and is proprietary to the American Chemical Society and its authors. Do not copy or disclose without written permission. If you have received this item in error, notify the sender and delete all copies.

**β-Cyclodextrin Polymers on Microcrystalline Cellulose as a Granular Media for Organic Micropollutant Removal from Water**

Journal:	<i>ACS Applied Materials &amp; Interfaces</i>
Manuscript ID	am-2018-22100t.R1
Manuscript Type:	Article
Date Submitted by the Author:	n/a
Complete List of Authors:	Alzate-Sánchez, Diego; Northwestern University, Chemistry Ling, Yuhan; Cornell University, Civil and Environmental Engineering Li, Chenjun; Cornell University, Civil and Environmental Engineering Frank, Benjamin; Johns Hopkins University, Chemistry Bleher, Reiner; Northwestern University, Department of Chemistry Fairbrother, D. Howard; Johns Hopkins University, Chemistry Helbling, Damian; Cornell University, School of Civil and Environmental Engineering Dichtel, William; Northwestern University, Department of Chemistry

**SCHOLARONE™**  
Manuscripts

# 1 2 3 4 5 6 7 8 9 10 11 12 13 14 15 16 17 18 19 20 21 22 23 24 25 26 27 28 29 30 31 32 33 34 35 36 37 38 39 40 41 42 43 44 45 46 47 48 49 50 51 52 53 54 55 56 57 58 59 60 β-Cyclodextrin Polymers on Microcrystalline Cellulose as a Granular Media for Organic Micropollutant Removal from Water

Diego M. Alzate-Sánchez,<sup>1</sup> Yuhang Ling,<sup>2</sup> Chenjun Li,<sup>2</sup> Benjamin P. Frank,<sup>3</sup> Reiner Bleher,<sup>4</sup>  
D. Howard Fairbrother,<sup>3,\*</sup> Damian E. Helbling,<sup>2,\*</sup> and William R. Dichtel<sup>1,\*</sup>

**Affiliations:** <sup>1</sup>Department of Chemistry, Northwestern University, Evanston, IL, 60208 USA;

<sup>2</sup>School of Civil and Environmental Engineering, Cornell University, Ithaca, NY, 14853 USA;

<sup>3</sup>Department of Chemistry, Johns Hopkins University, Baltimore, MD, 21218 USA; <sup>4</sup>Department  
of Materials Science and Engineering, Northwestern University, Evanston, IL, 60208 USA.

## KEYWORDS

β-Cyclodextrin, Cellulose, Micropollutants, Remediation, Water Treatment

## ABSTRACT

Organic contaminants at low concentrations, known as micropollutants, are a growing threat to water resources. Implementing novel adsorbents capable of removing micropollutants during packed-bed adsorption is desirable for rapid water purification and other efficient separations. We previously developed porous polymers based on cyclodextrins that demonstrated rapid uptake and high affinity for dozens of micropollutants (MPs) in batch experiments. However, these polymers are typically produced as powders with irregular particle size distributions in the range of tens of microns. In this powdered form, cyclodextrin polymers cannot be implemented in packed-bed adsorption processes because the variable particle sizes yield insufficient porosity and

1  
2  
3 consequently generate high back-pressure. Here we demonstrate a facile approach to remove  
4 micropollutants from water in a continuous manner by polymerizing cyclodextrin polymer  
5 networks onto cellulose microcrystals to provide a core/shell structure. Batch adsorption  
6 experiments demonstrate rapid pollutant uptake and high accessibility of the cyclodextrins on the  
7 adsorbent. Similarly, column experiments demonstrate rapid uptake of a model pollutant with  
8 minimal back-pressure, demonstrating potential for use in packed-bed adsorption processes.  
9 Furthermore, the pollutant-saturated columns were regenerated using methanol and reused three  
10 times with almost no change in performance. Column experiments conducted with a mixture of 15  
11 micropollutants at environmentally relevant concentrations demonstrated that removal was  
12 determined by the affinity of each micropollutant for cyclodextrin polymers. The cyclodextrin  
13 polymer grafted onto cellulose microcrystals is more resistant to both anaerobic and aerobic  
14 biodegradation as compared to cyclodextrins and unmodified cellulose crystals, presumably due  
15 to the aromatic crosslinkers, demonstrating durability. Collectively, the findings from this study  
16 demonstrate a general strategy to incorporate novel cyclodextrin adsorbents onto cellulose  
17 substrates to enable rapid and efficient removal of micropollutants during packed-bed adsorption,  
18 as well as their promising long-term stability and regeneration capabilities.  
19  
20  
21  
22  
23  
24  
25  
26  
27  
28  
29  
30  
31  
32  
33  
34  
35  
36  
37  
38  
39  
40  
41  
42  
43  
44  
45  
46  
47  
48  
49  
50  
51  
52  
53  
54  
55  
56  
57  
58  
59  
60

## INTRODUCTION

Humans introduce thousands of organic compounds, known as micropollutants (MPs) when present at trace concentrations, into ground and surface waters.<sup>1</sup> These MPs are substances used in agriculture, manufacturing, medicine, and other human activities.<sup>2</sup> Several studies have demonstrated that exposure to MPs may negatively influence both human health and aquatic ecosystems.<sup>3,4</sup> For example, the presence of bisphenol A (BPA), a suspected endocrine disruptor used to make plastics and epoxy resins, has raised concerns in human health because it can produce

1  
2  
3 adverse effects in mammary glands and the immune system at concentrations below its acute  
4 toxicity levels.<sup>5</sup>  
5  
6

7 Some polar and semi-polar MPs are stable and persistent in the environment, while others  
8 undergo biotic or abiotic transformation to form products that are persistent in water at trace  
9 concentrations, because they are only partially removed in conventional water treatment  
10 processes.<sup>6</sup> Therefore, enhanced treatments such as advanced oxidation, ultrafiltration, and  
11 adsorption are expected to play a role in MP removal, especially as the health and ecological effects  
12 of MPs are better understood.<sup>7-10</sup> Adsorption is a widely applicable technique because it can  
13 remove contaminants without introducing degradation byproducts,<sup>11</sup> and thus the scientific  
14 community has explored numerous materials for adsorption of contaminants in water.<sup>12,13</sup> The  
15 performance of such adsorbents have been evaluated in batch and/or packed-bed adsorption  
16 configurations.<sup>14,15</sup> Remediation of ground and drinking water relies in the use of granular  
17 adsorbents in packed-bed columns.<sup>16</sup> Therefore, the development of adsorbents to decontaminate  
18 water in a continuous setup is needed. Granular adsorbents have been employed to remove heavy  
19 metals and organic dyes from water in packed-bed columns.<sup>17,18</sup> However, the implementation of  
20 granular adsorbents capable of MP removal in packed-beds has not been addressed yet.  
21  
22

23 Adsorption capacity and fast mass transport are important characteristics for adsorbents  
24 developed for packed-bed adsorption processes.<sup>19</sup> However, the rate of adsorption and the mass  
25 transfer may become slow due to poor accessibility to the binding functional groups. To solve this  
26 problem development of core-shell adsorbents has been explored.<sup>20,21</sup> Furthermore, control of the  
27 adsorbent size and shape contributes to a rapid flow of water in packed-bed columns, which is  
28 desirable for continuous water remediation. Among the different materials explored as supports  
29 for sorbent deposition, cellulose possess the desired characteristics. Its hydroxyl groups allow  
30  
31  
32  
33  
34  
35  
36  
37  
38  
39  
40  
41  
42  
43  
44  
45  
46  
47  
48  
49  
50  
51  
52  
53  
54  
55  
56  
57  
58  
59  
60

1  
2  
3 reactions with different functional groups, producing covalent bonds between the adsorbent and  
4 the support.<sup>22</sup> Additionally, cellulose can be obtained in sizes ranging from tens of nanometers to  
5 hundreds of microns, and in different morphologies.<sup>23</sup> Finally, it is cheap, non-toxic and a green  
6 material. Consequently, cellulose is an outstanding material to support an adsorbent capable of  
7 removing MPs.  
8  
9

10  
11  
12  
13  
14  $\beta$ -cyclodextrin ( $\beta$ -CD) is an inexpensive and renewable carbohydrate produced from corn  
15 starch that forms host-guest complexes with thousands of organic compounds, including many  
16 micropollutants.<sup>24,25</sup> This property has led to the development of numerous  $\beta$ -CD-based  
17 adsorbents.<sup>26,27</sup> Moreover, cellulosic materials functionalized with  $\beta$ -CD have been proposed  
18 previously for the removal of pharmaceuticals from water. However, the particle size of the  
19 proposed adsorbent is not suitable for packed-bed adsorption, and only relatively untunable  
20 monomeric  $\beta$ -CDs were employed.<sup>28</sup> We recently reported the first permanently porous  $\beta$ -CD  
21 polymer network, which was obtained by crosslinking  $\beta$ -CD with tetrafluoroterephthalonitrile  
22 (TFN) via a nucleophilic aromatic substitution.<sup>29</sup> The  $\beta$ -CD polymer removes pollutants more  
23 quickly and effectively than coconut shell activated carbon, is easily regenerated, and is not fouled  
24 by humic acids, a major constituent of natural organic matter.<sup>30</sup> However, when packed into  
25 columns, its particle size and morphology limit the water flux, preventing the evaluation of its  
26 performance in column experiments that simulate packed-bed adsorption processes. Here we  
27 polymerize a  $\beta$ -CD polymer onto the surface of 100  $\mu$ m long rod-like cellulose microcrystals,  
28 using the knowledge gained in our previous report of forming the  $\beta$ -CD polymer on cotton fabrics  
29 to remove volatile organic compounds.<sup>31</sup> Batch adsorption of Bisphenol A (BPA) demonstrates  
30 that the polymer retains its binding characteristics in this form. Moreover, the modified  
31 microcrystals were packed into columns that generated comparable back pressure to the  
32  
33  
34  
35  
36  
37  
38  
39  
40  
41  
42  
43  
44  
45  
46  
47  
48  
49  
50  
51  
52  
53  
54  
55  
56  
57  
58  
59  
60

1  
2  
3 unmodified microcrystals, and exhibit even faster MP adsorption compared to the unsupported  
4 polymer. We also demonstrate the in-situ regeneration and reusability of the new material, and its  
5 performance in removing a mixture of fifteen micropollutants at environmentally relevant  
6 concentrations in column experiments. Finally, the biodegradability of the polymer is tested under  
7 anaerobic and aerobic conditions. These combined observations demonstrate the utility and  
8 durability of the  $\beta$ -CD polymer for MP removal from water.  
9  
10  
11  
12  
13  
14  
15

## 17 RESULTS AND DISCUSSION

### 18 Synthesis and Characterization

21 Polymerization of the  $\beta$ -CD polymer onto cellulose microcrystals (CMCs) was performed by  
22 combining  $\beta$ -CD, TFN, CMCs, and  $K_2CO_3$  in a solvent mixture of DMSO:H<sub>2</sub>O (7:3 v/v) at 85 °C  
23 for 24 h (Figure 1). These conditions were adapted from a recent mechanistic study of the  
24 polymerization<sup>32</sup> and those used to graft the  $\beta$ -CD polymer onto cotton.<sup>31</sup> The solid recovered under  
25 these reaction conditions provided the highest yield and exhibited the highest capacity for  
26 adsorbing bisphenol A (BPA) (Figure S1). However, scanning electron microscopy (SEM, Figure  
27 2a) indicated that the solid was a physical mixture of small particles later assigned as the  $\beta$ -CD  
28 homopolymer (CD-TFN) and larger particles that were CMCs with CD-TFN grafted to their  
29 surfaces (CD-TFN@CMC). These populations were separated by sieving using a 45  $\mu$ m mesh,  
30 and then characterized by SEM and powder X-ray diffraction (PXRD). The CD-TFN  
31 homopolymer is amorphous, whereas CMCs exhibit a characteristic powder pattern of crystalline  
32 cellulose. Cellulose diffraction peaks are prominent in both the as-synthesized sample (Figure 2A)  
33  
34  
35  
36  
37  
38  
39  
40  
41  
42  
43  
44  
45  
46  
47  
48  
49  
50  
51  
52  
53  
54  
55  
56  
57  
58  
59  
60

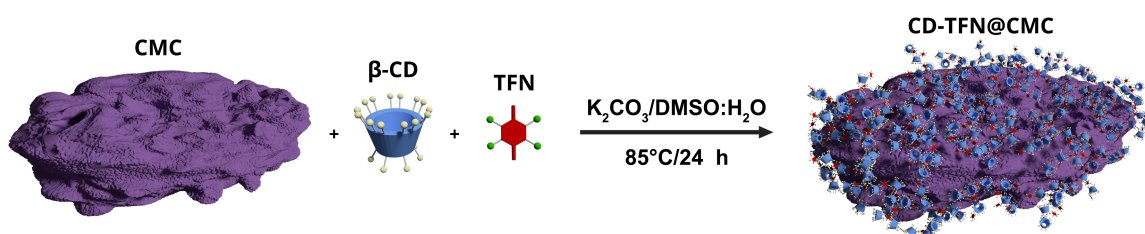


**Figure 1.** Reaction scheme of the CD-TFN@CMC synthesis.

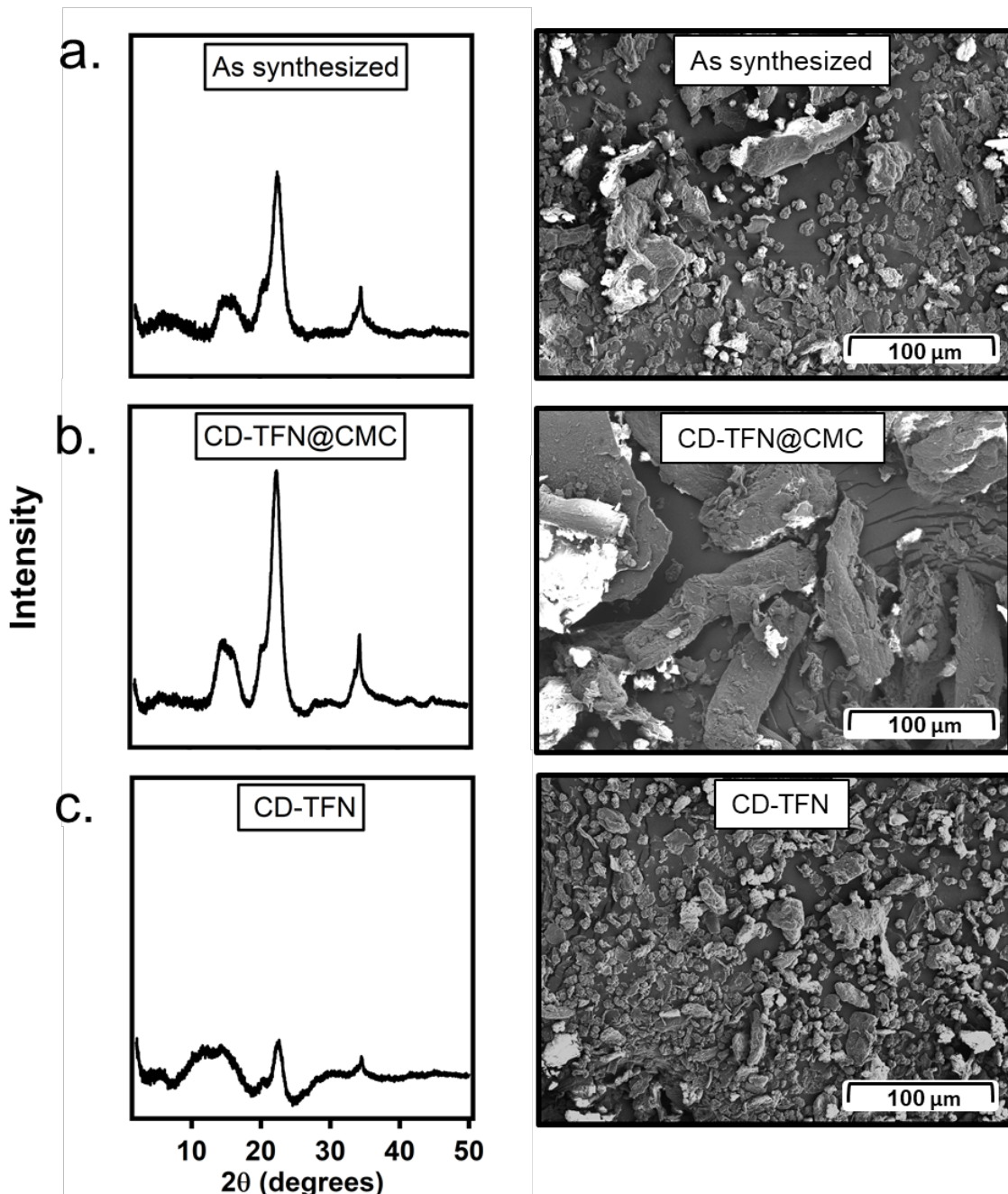


**Figure 2.** PXRD data (left) and SEM images (right) of (a) the crude solid isolated from the precipitation, (b) the solid retained by the sieve (predominantly CD-TFN@CMC), and (c) solid passed by the sieve (CD-TFN).

1  
2  
3 and in the larger particles retained on the sieve (Figure 2B). However, these peaks are relatively  
4 faint in the diffraction pattern obtained from the particles that passed through the sieve (Figure  
5 2C), indicating that these particles contain fewer CMCs. SEM images of the larger particles after  
6 sieving confirmed that CD-TFN@CMC retained their original morphology and size, suggesting  
7 negligible crosslinking between CMC particles by the  $\beta$ -CD polymer (Figure 2B), while the CD-  
8 TFN sample consisted of particles with smaller size and rounded morphology (Figure 2C). The  
9 separated CD-TFN@CMC and CD-TFN samples were each evaluated for their micropollutant  
10 removal performance and compatibility with column designs.  
11  
12

13 Fourier-transform infrared spectroscopy (FTIR) and surface composition analysis of the  
14 sieved CD-TFN and CD-TFN@CMC samples were consistent with the expected structures.  
15 Notably, the FTIR spectra of the two materials are similar because both  $\beta$ -CD and cellulose are  
16 comprised of 1,4-linked glucose units, and no significant differences in the position of the FTIR  
17 absorption bands were observed after sieving (Figure S2). The spectra exhibit typical bands for  
18 carbohydrates (O-H stretching and C-O stretching at 3400 and 1025  $\text{cm}^{-1}$ , respectively) and the  
19 C≡N stretches and C=C stretches of the TFN groups at 2240 and 1475  $\text{cm}^{-1}$ , respectively.<sup>29,33</sup> X-  
20 ray photoelectron spectroscopy (XPS) of CD-TFN and CD-TFN@CMC indicated the presence of  
21 both nitrogen and fluorine, confirming the incorporation of the crosslinker, whereas spectra of  
22 unmodified CMCs show no N or F signals (Figure S3). These combined observations indicate that  
23 the  $\beta$ -CD polymer is present on the surface of CMCs in the CD-TFN@CMC sample.  
24  
25

26 Combustion analysis and powder X-ray diffraction (PXRD) were used to estimate the  
27 loading of the  $\beta$ -CD polymer in the CD-TFN@CMC sample. The amount of CMC in CD-  
28 TFN@CMC and CD-TFN was calculated from the PXRD spectra. We determined a loading of  
29 78.6  $\pm$  1.9 wt% of CMC in CD-TFN@CMC. In contrast, 22.2  $\pm$  0.7 wt% residual CMC in the CD-  
30  
31  
32  
33  
34  
35  
36  
37  
38  
39  
40  
41  
42  
43  
44  
45  
46  
47  
48  
49  
50  
51  
52  
53  
54  
55  
56  
57  
58  
59  
60

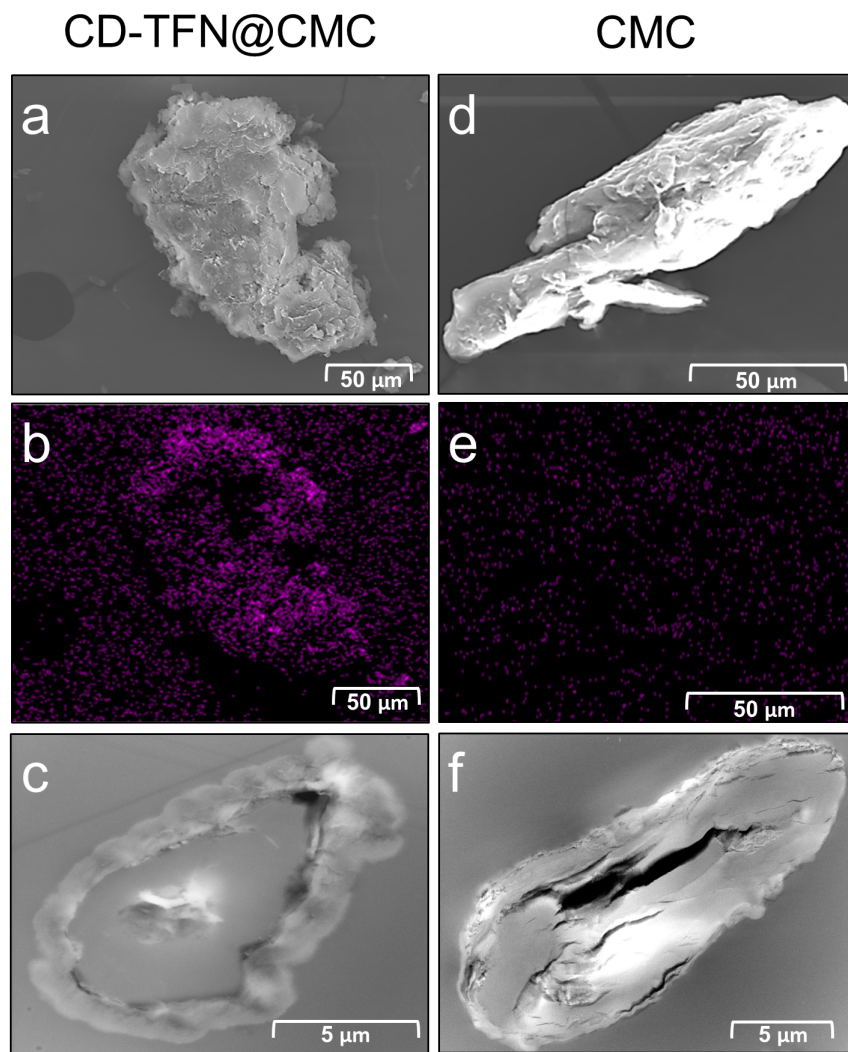
TFN homopolymer was found, indicating that some CMC particles passed through the sieve (see the SI for detailed calculations). The N content of each sample obtained from combustion analysis provided an estimate of  $28.1 \pm 0.2$  and  $12.4 \pm 0.5$  wt% TFN for CD-TFN and CD-TFN@CMC respectively. The combination of PXRD and combustion analysis were used to estimate that the  $\beta$ -CD content in the CD-TFN homopolymer and CD-TFN@CMC was  $50.4 \pm 0.7$  and  $11.6 \pm 1.9$  wt%, respectively. Based on the F content of the samples, we calculated a TFN: $\beta$ -CD molar ratio of  $3.2 \pm 0.05$  and  $6.1 \pm 1.0$  for CD-TFN and CD-TFN@CMC and an average degree of substitution of the TFN of  $2.9 \pm 0.03$  and  $2.7 \pm 0.05$ , respectively (Table 1). These combined results indicate more TFN per  $\beta$ -CD in CD-TFN@CMC, although some of these crosslinkers are likely to be attached to the glucose subunits of the cellulose microcrystals. Nevertheless, the inherent reactivity of TFN is similar to the CD-TFN homopolymer, since the average degree of substitution is similar for the two samples. The overall bulk compositional analysis indicates that CD-TFN@CMC contains approximately 21.4 wt% of the  $\beta$ -CD polymer covalently bound to the cellulose microcrystals.

**Table 1.** Composition of CD-TFN@CMC and CD-TFN samples calculated from PXRD and elemental analysis results.

	CMC (wt%)	$\beta$ -CD (wt%)	TFN (wt%)	$\beta$ -CD (mmol/g)	TFN: $\beta$ -CD molar ratio	TFN substitution
CD-TFN@CMC	$78.6 \pm 1.9$	$11.6 \pm 1.9$	$12.4 \pm 0.5$	$10.2 \pm 1.7$	$6.1 \pm 1.0$	$2.9 \pm 0.03$
CD-TFN	$22.2 \pm 0.7$	$50.4 \pm 0.7$	$28.1 \pm 0.2$	$44.4 \pm 0.6$	$3.2 \pm 0.05$	$2.7 \pm 0.05$

Elemental mapping using energy dispersive spectroscopy (EDS) demonstrates that the  $\beta$ -CD polymer is found on the surface of CMC in the CD-TFN@CMC sample. In the fluorine mapping image, higher counts are homogeneously distributed around the CMC particles, corresponding to the presence of the TFN groups (Figure 3b). The CD-TFN homopolymer

1  
2  
3 particles show a similar fluorine signal (Figure S5), whereas unmodified CMC shows no fluorine  
4  
5 (Figure 3e), but both particles show carbon and oxygen (Figure S4). The CD-TFN on the surface  
6  
7 of the CMCs was visualized with excellent contrast using scanning transmission electron  
8  
9 microscopy (STEM). The CD-TFN@CMC particles were



49  
50  
51  
52  
53  
54  
55  
56  
57  
58  
59  
60 **Figure 3.** (a) Scanning electron micrograph, (b) fluorine mapping, and (c) cross sectional STEM  
of CD-TFN@CMC; (d) scanning electron micrograph, (e) fluorine mapping, and (f) cross sectional  
STEM of unmodified CMC. The cross-sectional images were obtained by embedding the samples  
in a methacrylate resin, which was cured, microtomed, and imaged.

1  
2  
3 dispersed into a methacrylate resin, cured, microtomed to 200 nm-thick sections, and analyzed by  
4 STEM. The cross-sectional image (Figure 3c) reveals a core surrounded by a shell. Unmodified  
5 CMC subjected to the same analysis do not show a shell-like structure (Figure 3f). The thickness  
6 of the  $\beta$ -CD polymer shell is  $1.50 \pm 0.39 \mu\text{m}$  (Figure S6), which is smaller than the average particle  
7 size of the CD-TFN homopolymer ( $>10$  microns, Figure S7). These findings indicate the  
8 formation of the  $\beta$ -CD polymer as a thin coating around the cellulose in CD-TFN@CMC.  
9  
10  
11  
12  
13  
14  
15  
16

## 2.2 Bisphenol A Uptake in Batch Experiments

17  
18 We performed batch isotherm experiments with CD-TFN, CD-TFN@CMC, and CMC to  
19 determine the adsorption capacity of each material for BPA. Isotherm experiments were conducted  
20 with 1 mg adsorbent per mL of solution and with initial BPA concentrations ranging from 0.1 to  
21 1 mM. The results are presented in Figure 4a and Figure S8. We used the Langmuir isotherm  
22 model (Equation S8) to estimate the maximum adsorption capacity ( $q_{\max}$ ) in terms of mg BPA/g  
23 adsorbent and mg BPA/g  $\beta$ -CD (Figure S8,S9 and Table S1).<sup>34</sup>  
24  
25

26 CMC exhibited limited BPA removal in all experiments, and no fit was possible to the  
27 Langmuir isotherm. CD-TFN and CD-TFN@CMC both exhibited significant uptake of BPA and  
28 Langmuir isotherms were developed. We found that the  $q_{\max}$  for CD-TFN is  $193.6 \pm 7.8$  mg BPA/g  
29 solid, which corresponds to a combination of specific (formation of an inclusion complex with  $\beta$ -  
30 CD) and nonspecific (interaction with the crosslinker and pores of the network) BPA adsorption.<sup>29</sup>  
31 The maximum BPA capacity for CD-TFN@CMC is  $34.7 \pm 1.6$  mg BPA/g solid. We found that  
32 the capacity of the adsorbents per unit mass of  $\beta$ -CD for CD-TFN and CD-TFN@CMC are  $384.2$   
33  $\pm 31.6$  mg BPA/g  $\beta$ -CD and  $299.1 \pm 27.3$  mg BPA/g  $\beta$ -CD respectively (Figure S8, Table S1),  
34 which indicates that CD-TFN and CD-TFN@CMC have similar capacity per unit mass of  $\beta$ -CD.  
35 Uptake values of the adsorbents demonstrate that  $\beta$ -CD is present in CD-TFN and CD-  
36  
37  
38  
39  
40  
41  
42  
43  
44  
45  
46  
47  
48  
49  
50  
51  
52  
53  
54  
55  
56  
57  
58  
59  
60

TFN@CMC, and it is completely available to form inclusion complexes with micropollutants like BPA, which is an important characteristic to maximize adsorbent performance.

We also measured the kinetics of BPA uptake in batch experiments conducted with 1 mg/mL polymer loading and  $[BPA] = 0.1$  mM. The results demonstrate that CD-TFN@CMC removes BPA more quickly than CD-TFN itself (Figure 4b). CD-TFN reaches its equilibrium uptake of BPA within 2 min, which is comparable to our previous reports.<sup>29,30</sup> CD-TFN@CMC reaches equilibrium within 20 seconds under identical conditions. The relative kinetics of adsorbents with different capacities may be compared directly by calculating a parameter known as relaxation time ( $t_r$ ), with shorter times corresponding to more rapid micropollutant binding (see Supporting Information for details of the calculation).<sup>35</sup> The  $t_r$  of CD-TFN and CD-TFN@CMC

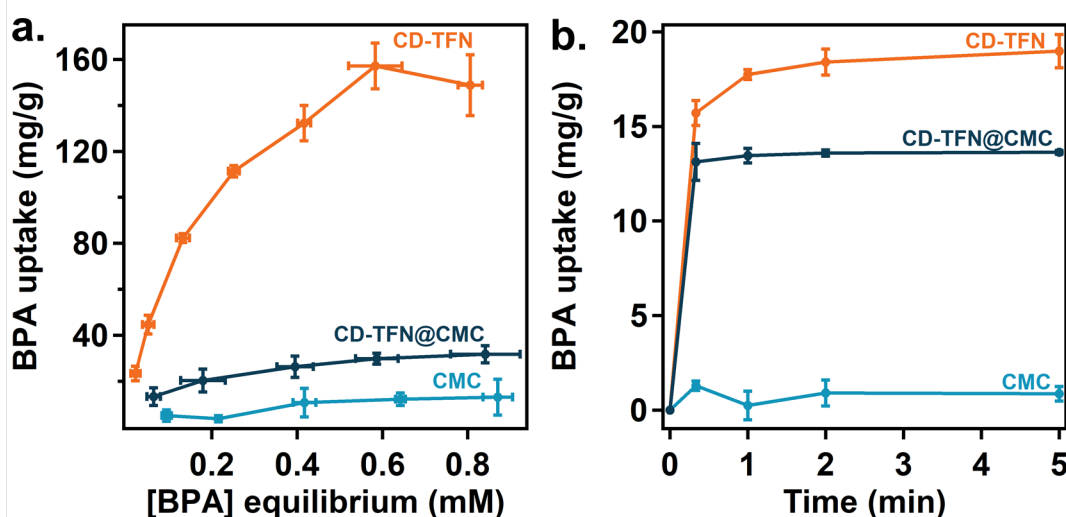


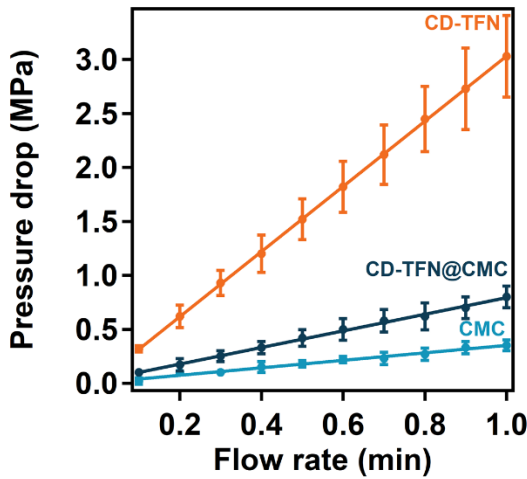
**Figure 4.** (a) BPA uptake of CMC, CD-TFN and CD-TFN@CMC as a function of the equilibrium BPA concentration (1 mg of solid/mL of solution, measured at equilibrium), and (b) BPA uptake by CMC, CD-TFN and CD-TFN@CMC and as a function of time (1 mg of solid/mL of solution,  $[BPA]_0=0.1$  mM).

1  
2  
3 are  $3.75 \pm 0.50$  s and  $0.89 \pm 0.03$ , respectively (Figure S10 and Table S1). We conclude that CD-  
4  
5 TFN@CMC's rapid BPA uptake occurs because the formation of a thin outer layer of polymer in  
6 the CMCs, and the highly accessible network of  $\beta$ -CD polymers crosslinked with TFN,<sup>29</sup> such that  
7  
8 BPA can rapidly access the  $\beta$ -CD binding sites. This rapid uptake suggests outstanding potential  
9 for implementing CD-TFN@CMC in packed-bed adsorption processes.  
10  
11

### 12 2.3 Permeability Test

13  
14

15 Because of CD-TFN@CMC's larger particle size, packed columns exhibit significantly lower back  
16 pressure than those prepared from the CD-TFN homopolymer. Back pressure in packed columns  
17 depends on particle size, morphology, and distribution, and thus large, homogenous particles are  
18 desirable.<sup>36</sup> CD-TFN has an irregular shape and a broad size distribution, while CD-TFN@CMC  
19 has a size distribution centered at 100  $\mu$ m. Chromatography columns were packed with equal  
20 masses of CD-TFN@CMC, CD-TFN, or CMC and connected to a liquid chromatography (LC)  
21  
22  
23  
24  
25  
26  
27  
28  
29  
30  
31  
32  
33



50 **Figure 5.** Back pressure as a function of flow rate for CMC, CD-TFN, and CD-TFN@CMC  
51 packed in liquid chromatographic columns, using water as the mobile phase, and 200 mg of  
52 adsorbent.  
53  
54  
55

1  
2  
3 pump to measure back pressure as a function of flow rate. CD-TFN@CMC had only slightly higher  
4 back pressure than unmodified CMC (Figure 5), and CD-TFN had much higher back pressure.  
5  
6 This higher permeability, combined with its rapid uptake, makes CD-TFN@CMC a promising  
7 candidate for implementing CD-TFN@CMC in packed-bed adsorption processes.  
8  
9

#### 10 2.4 Bisphenol A Uptake in Column Experiments

11  
12 A chromatography column was packed with 200 mg of CD-TFN@CMC and used to evaluate the  
13 removal of BPA from water. The column was subjected to breakthrough tests using BPA solutions  
14 of varying concentrations (0.1, 0.5 and 1.0 mM). The CD-TFN@CMC column exhibits  
15 breakthrough volumes that depended non-linearly on BPA concentration (Figure 6a). By contrast,  
16 columns packed with CMC showed more rapid breakthrough that was independent of BPA  
17 concentration, indicating that CMC does not remove BPA from water (Figure S11). Furthermore,  
18 the amount of BPA adsorbed in each experiment is similar to the quantity measured in batch  
19 experiments (Figure S12). This finding indicates that the capacity of the adsorbent is not affected  
20 when is tested in a continuous adsorption setup and demonstrates that batch adsorption can be used  
21 to predict the behavior of CD-TFN@CMC in column experiments. Finally, the CD-TFN@CMC  
22 column was saturated with a 1.0 mM BPA solution and regenerated by in situ washing with  
23  $\text{CH}_3\text{OH}$  and re-equilibrating with clean  $\text{H}_2\text{O}$ . After three adsorption/regeneration cycles, the  
24 capacity and breakthrough time of the column were unchanged (Figure 6b). These breakthrough  
25 and regeneration experiments support the use of CD-TFN@CMC in packed-bed adsorption  
26 processes and motivate further experiments at environmentally relevant concentrations.  
27  
28  
29  
30  
31  
32  
33  
34  
35  
36  
37  
38  
39  
40  
41  
42  
43  
44  
45  
46  
47  
48  
49  
50  
51  
52  
53  
54  
55  
56  
57  
58  
59  
60

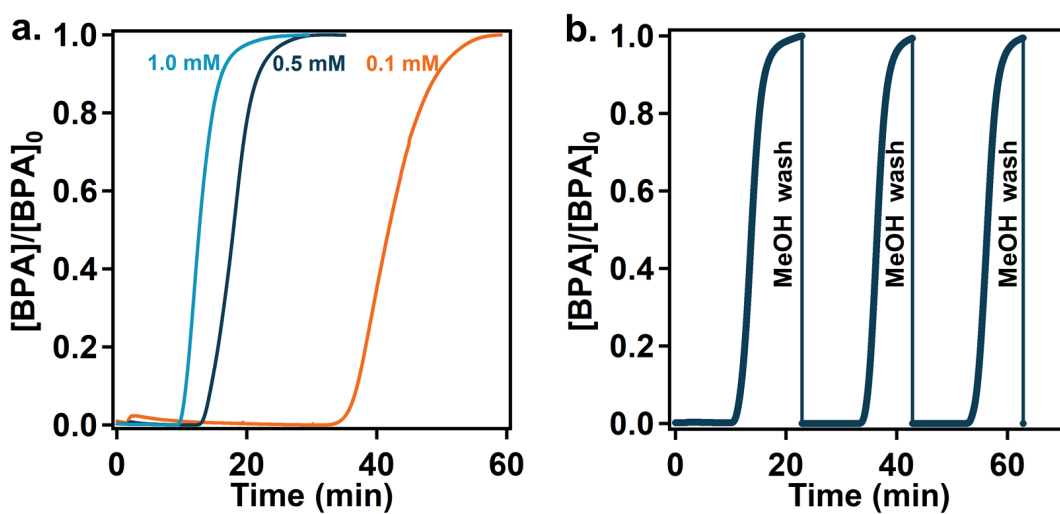
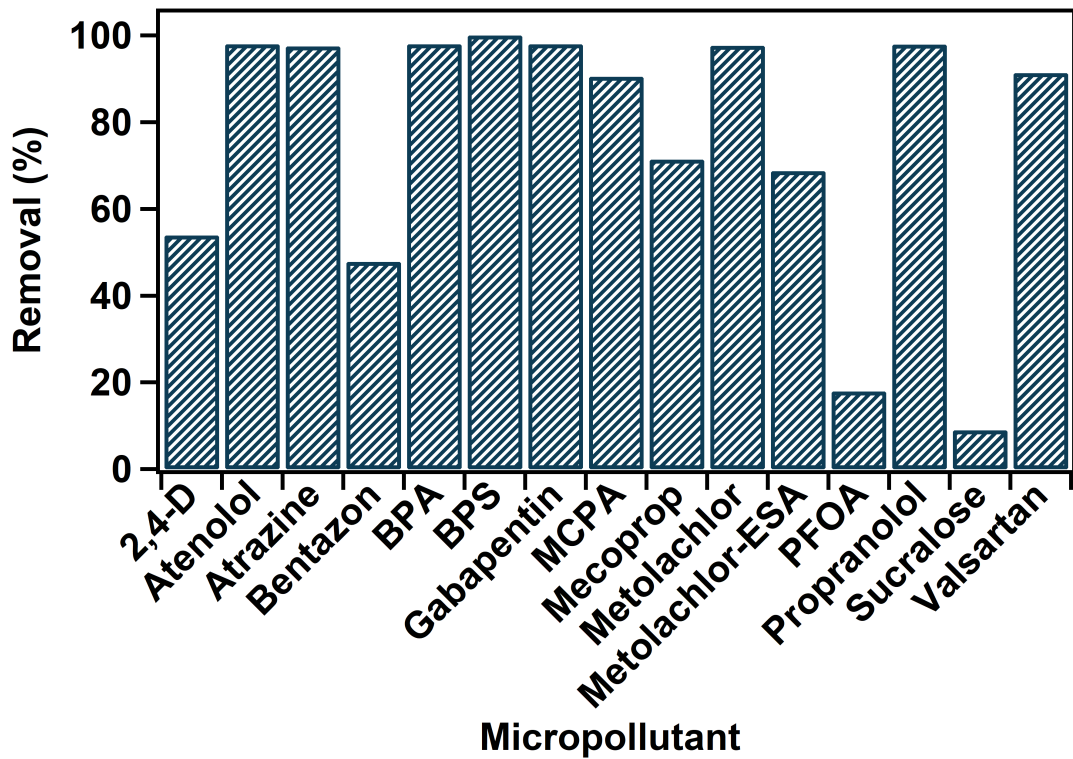


**Figure 6.** (a) Packed-bed uptake of BPA at three different BPA concentrations, measured as a function of time for CD-TFN@CMC (200 mg) packed in a column, and (b) Packed-bed regeneration of CD-TFN@CMC (200 mg) packed in a column. Saturation was performed with a 1.0 mM BPA solution and methanol was used for regeneration.

A column packed with 200 mg of CD-TFN@CMC also removes MPs at environmentally relevant concentrations. We selected 15 MPs that exhibited varying affinity for CD-TFN in previous batch experiments and prepared a mixture containing  $10 \mu\text{g L}^{-1}$  of each MP.<sup>30</sup> We designed a series of column experiments to evaluate the removal of the 15 MPs from water (see SI for experimental details). The results of the experiments are presented in Figure 7. Seven MPs exhibited complete removal over the duration of the 60 minute experiment; these MPs also exhibited the greatest affinity for CD-TFN in previous batch experiments ( $\log K_D > 0.3$ ).<sup>30,32</sup> The remaining MPs exhibited varying levels of removal over the duration of the experiment, and we report the total removal calculated by taking the area above the breakthrough curve as described in the SI and summarized in Figure 7, Figure S13 and Figure S14. Two compounds (sucralose and PFOA) exhibited complete breakthrough within the 60 minute duration of the experiment, and the

1  
2  
3 remaining MPs that were partially removed exhibited varying degrees of breakthrough within 60  
4 minutes. The  $K_D$  values of the partially removed MPs are also proportional to their removal levels  
5 in the column experiments. Based on these experiments, we conclude that CD-TFN@CMC  
6 removes MPs in column experiments to varying degrees that correlate significantly with their  $K_D$   
7 values measured in batch reactors (t-test,  $p < 0.00001$ ). Therefore, the removal of other MPs by CD-  
8 TFN@CMC should also be predictable based on their affinity observed in batch experiments.  
9  
10  
11  
12  
13  
14  
15



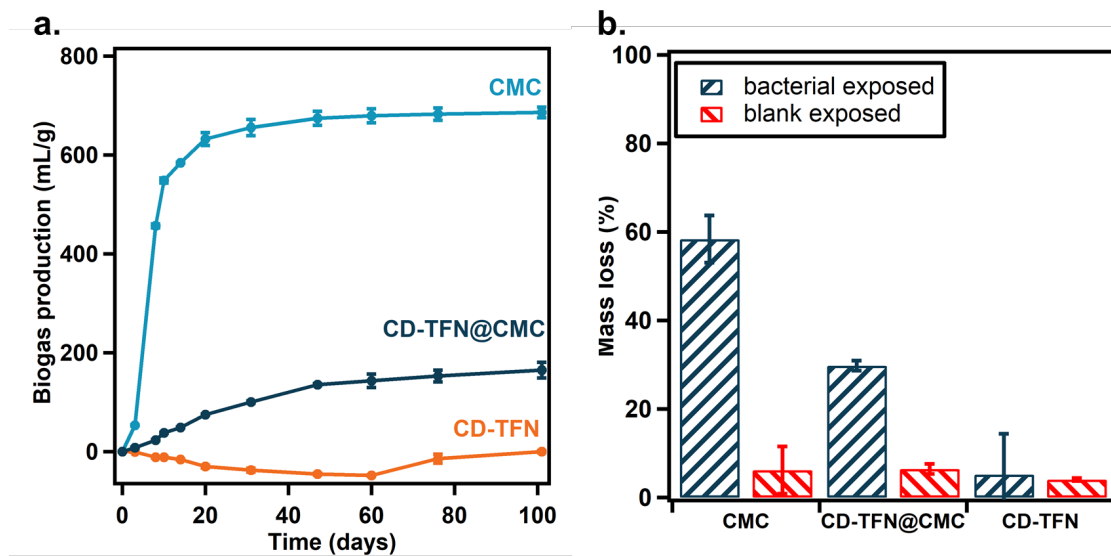
45  
46 **Figure 7.** Packed-bed adsorption of 15 MPs (10 ppb each) by CD-TFN@CMC packed in a column  
47 (200 mg). Flow rate was 0.2 mL/min. Removal was calculated as the ratio of the area above the  
48 breakthrough curve over the total area from 0 to 60 min.  
49  
50  
51  
52  
53  
54  
55  
56  
57  
58  
59  
60

## 2.5 Stability Towards Biodegradation

The CD-TFN homopolymer shows excellent stability to microorganisms under both anaerobic and aerobic conditions. CD-TFN@CMC is partially biodegradable, which we attribute to the  $\beta$ -CD polymer coating that slows down the degradation of the CMC core. The anaerobic biodegradation of the materials was characterized by monitoring their biogas production in an anaerobic bioreactor for 103 days. Unmodified CMC (Figure 8a) and  $\beta$ -CD (Figure S15) are degraded by the mixed culture anaerobic bacteria as tracked by their mineralization into biogas, which plateaus at 40 days. In contrast, the biogas production for CD-TFN remained at baseline levels for the duration of the experiment, indicating that it is not biodegradable by virtue of the TFN crosslinker (Figure S15). CD-TFN@CMC produced biogas above baseline levels, which ceased after 60 days. However, its biodegradation is slower and less extensive than CMC itself. We attribute these observations to the  $\beta$ -CD polymer coating limiting the rate and extent of CMC biodegradation.

CD-TFN also resists degradation, and CD-TFN@CMC is partially stable under aerobic conditions, which was assessed by monitoring mass decreases after 46 days of incubation in the presence of aerobic mixed culture bacteria. CMC exhibited the greatest mass loss in aerobic media and is therefore biodegradable in both environments. CD-TFN again showed no bacterial degradation, and CD-TFN@CMC showed partial degradation (Figure 8b). CD-TFN@CMC showed no difference in its BPA uptake capacity after blank (no bacteria) and bacterial aging (Figure S16). Additionally, SEM images of the aged samples reveal no differences in the morphology or the particle size of the adsorbents (Figure S17). Based on these observations, the partial biodegradability of CD-TFN@CMC likely comes from gaps on the CMC surface that were not coated by the polymer. Based on these experiments, we anticipate that CD-TFN@CMC will show superior stability to aerobic bacterial aging during water remediation compared to cellulose-

1  
2  
3 based materials without a protecting layer. The extent of this stabilization will depend on the nature  
4  
5 of the  $\beta$ -CD polymer coating in an optimized application-specific form.  
6  
7



28 **Figure 8.** (a) Biogas production per unit mass of CMC, CD-TFN@CMC and CD-TFN as a  
29 function of time in an anaerobic environment, and (b) mass loss during aerobic degradation of  
30 CMC, CD-TFN@CMC, and CD-TFN.  
31  
32

## 33 CONCLUSIONS

34 Cellulose is a natural support for cross-linked cyclodextrin polymers because it is inexpensive,  
35 available in many morphologies and sizes, and its hydroxyl groups participate in polymerizations  
36 alongside those of  $\beta$ -CD itself. CD-TFN polymers have shown excellent affinity and superior  
37 kinetics compared to activated carbons in previous reports, but its native particle size and  
38 morphology preclude leveraging these desirable properties for water treatment during packed-bed  
39 adsorption. Here we have used CMC as a support for CD-TFN to obtain an adsorbent with a  
40 core/shell structure, with similar adsorption efficiency as the native material, fast kinetics, and low  
41 back pressure when packed into columns. These characteristics enabled the first breakthrough  
42

1  
2  
3 experiments of CD-TFN adsorbents. The columns were amenable to regeneration with no observed  
4 performance loss. Column experiments with pollutant mixtures with varying affinity to CD-TFN  
5 at environmentally relevant concentrations, indicated complete removal of high-affinity MPs and  
6 selectivity consistent with previous batch studies. CD-TFN and CD-TFN@CMC showed  
7 significant resistance to biodegradation despite their high carbohydrate content, which we attribute  
8 to their heavy TFN cross-linking and core-shell structure of CD-TFN@CMC. Overall, this work  
9 represents a significant step forward towards leveraging the desirable characteristics of  
10 cyclodextrin adsorbents for removing micropollutants from impacted water resources. This  
11 approach represents an important step in developing high-performance and economical granular  
12 forms of  $\beta$ -CD polymers, as future developments will focus on methods that produce granular  
13 materials exclusively.  
14

15 ASSOCIATED CONTENT  
16  
17

## 18 ASSOCIATED CONTENT

19 **Supporting Information.** The Supporting Information is available free of charge on the ACS  
20 Publications website at DOI:  
21  
22

23  
24  
25  
26  
27  
28  
29  
30  
31  
32  
33  
34  
35  
36  
37  
38  
39  
40  
41  
42  
43  
44  
45  
46  
47  
48  
49  
50  
51  
52  
53  
54  
55  
56  
57  
58  
59  
60  
AUTHOR INFORMATION

## Corresponding Authors

W. R. Dichtel: wdichtel@northwestern.edu

D. E. Helbling: damian.helbling@cornell.edu

D. H. Fairbrother: howardf@jhu.edu

## Notes

The authors declare the following competing financial interest(s): W.R.D. And D.E.H. own equity

1  
2  
3 and or stock options in CycloPure Inc., which is commercializing materials related to those  
4 reported in this work.  
5  
6

7  
8  
9 **ACKNOWLEDGEMENT**  
10  
11

12 This work was supported by the National Science Foundation (NSF) through the Center for  
13 Sustainable Polymers (CHE-1413862). This work made use of the IMSERC, and NUANCE  
14 facilities at Northwestern University, which have received support from the Soft and Hybrid  
15 Nanotechnology Experimental (SHyNE) Resource (NSF ECCS-1542205); the State of Illinois and  
16 International Institute for Nanotechnology (IIN). This work was also supported by the National  
17 Science Foundation under the Center for Sustainable Nanotechnology (CSN), CHE-1503408. The  
18 Center for Sustainable Polymers and the Center for Sustainable Nanotechnology are part of the  
19 NSF Centers for Chemical Innovation Program.  
20  
21  
22  
23  
24  
25  
26  
27  
28  
29  
30

31 **REFERENCES**  
32  
33

34 (1) Pye, V. I.; Patrick, R. Ground Water Contamination in the United States. *Science* **1983**, 221  
35 (4612), 713–718.  
36  
37 (2) Schwarzenbach, R. P.; Egli, T.; Hofstetter, T. B.; von Gunten, U.; Wehrli, B. Global Water  
38 Pollution and Human Health. *Annu. Rev. Environ. Resour.* **2010**, 35 (1), 109–136.  
39  
40 (3) Melzer, D.; Rice, N.; Depledge, M. H.; Henley, W. E.; Galloway, T. S. Association between  
41 Serum Perfluorooctanoic Acid (PFOA) and Thyroid Disease in the U.S. National Health  
42 and Nutrition Examination Survey. *Environ. Health Perspect.* **2010**, 118 (5), 686–692.  
43  
44 (4) Kim, S.; Aga, D. S. Potential Ecological and Human Health Impacts of Antibiotics and  
45 Antibiotic-Resistant Bacteria from Wastewater Treatment Plants. *J. Toxicol. Environ. Heal.*  
46  
47  
48  
49  
50  
51  
52  
53  
54  
55  
56  
57  
58  
59  
60

1  
2  
3      *Part B* **2007**, *10* (8), 559–573.  
4  
5

6      (5) Vandenberg, L. N.; Colborn, T.; Hayes, T. B.; Heindel, J. J.; Jacobs, D. R.; Lee, D.-H.;  
7      Shioda, T.; Soto, A. M.; vom Saal, F. S.; Welshons, W. V.; Zoeller, R. T.; Myers, J. P.  
8      Hormones and Endocrine-Disrupting Chemicals: Low-Dose Effects and Nonmonotonic  
9      Dose Responses. *Endocr. Rev.* **2012**, *33* (3), 378–455.  
10  
11  
12  
13  
14  
15  
16      (6) Schwarzenbach, R. P.; Escher, B. I.; Fenner, K.; Hofstetter, T. B.; Johnson, C. A.; von  
17      Gunten, U.; Wehrli, B. The Challenge of Micropollutants in Aquatic Systems. *Science* **2006**,  
18      *313* (5790), 1072–1077.  
19  
20  
21  
22  
23  
24      (7) Comminellis, C.; Kapalka, A.; Malato, S.; Parsons, S. A.; Poulios, I.; Mantzavinos, D.  
25      Advanced Oxidation Processes for Water Treatment: Advances and Trends for R&D. *J.*  
26      *Chem. Technol. Biotechnol.* **2008**, *83* (6), 769–776.  
27  
28  
29  
30  
31      (8) Pendergast, M. M.; Hoek, E. M. V. A Review of Water Treatment Membrane  
32      Nanotechnologies. *Energy Environ. Sci.* **2011**, *4* (6), 1946–1971.  
33  
34  
35  
36  
37      (9) Worch, E. *Adsorption Technology in Water Treatment: Fundamentals, Processes, and*  
38      *Modeling*; De Gruyter: Berlin, Boston, 2012.  
39  
40  
41  
42      (10) Luo, Y.; Guo, W.; Ngo, H. H.; Nghiem, L. D.; Hai, F. I.; Zhang, J.; Liang, S.; Wang, X. C.  
43      A Review on the Occurrence of Micropollutants in the Aquatic Environment and Their Fate  
44      and Removal during Wastewater Treatment. *Sci. Total Environ.* **2014**, *473–474*, 619–641.  
45  
46  
47  
48  
49  
50      (11) Ali, I.; Gupta, V. K. Advances in Water Treatment by Adsorption Technology. *Nat. Protoc.*  
51      **2007**, *1* (6), 2661–2667.  
52  
53  
54  
55  
56      (12) Mohammed, N.; Grishkewich, N.; Tam, K. C. Cellulose Nanomaterials: Promising  
57  
58  
59

1  
2  
3 Sustainable Nanomaterials for Application in Water/Wastewater Treatment Processes.  
4  
5 *Environ. Sci. Nano* **2018**, *5* (3), 623–658.  
6  
7

8  
9 (13) Sweetman, M.; May, S.; Mebberson, N.; Pendleton, P.; Vasilev, K.; Plush, S.; Hayball, J.  
10  
11 Activated Carbon, Carbon Nanotubes and Graphene: Materials and Composites for  
12  
13 Advanced Water Purification. *C* **2017**, *3* (4), 18–47.  
14  
15  
16 (14) Liu, Z.; Wang, H.; Liu, C.; Jiang, Y.; Yu, G.; Mu, X.; Wang, X. Magnetic Cellulose–  
17  
18 chitosan Hydrogels Prepared from Ionic Liquids as Reusable Adsorbent for Removal of  
19  
20 Heavy Metal Ions. *Chem. Commun.* **2012**, *48* (59), 7350.  
21  
22  
23 (15) Goodman, S. M.; Bura, R.; Dichiara, A. B. Facile Impregnation of Graphene into Porous  
24  
25 Wood Filters for the Dynamic Removal and Recovery of Dyes from Aqueous Solutions.  
26  
27 *ACS Appl. Nano Mater.* **2018**, *1* (10), 5682–5690.  
28  
29  
30 (16) Ali, I. Water Treatment by Adsorption Columns: Evaluation at Ground Level. *Sep. Purif.*  
31  
32 *Rev.* **2014**, *43* (3), 175–205.  
33  
34  
35 (17) d’Halluin, M.; Rull-Barrull, J.; Bretel, G.; Labrugère, C.; Le Grogne, E.; Felpin, F.-X.  
36  
37 Chemically Modified Cellulose Filter Paper for Heavy Metal Remediation in Water. *ACS*  
38  
39  
40 *Sustain. Chem. Eng.* **2017**, *5* (2), 1965–1973.  
41  
42  
43  
44 (18) Mohammed, N.; Grishkewich, N.; Waeijen, H. A.; Berry, R. M.; Tam, K. C. Continuous  
45  
46 Flow Adsorption of Methylene Blue by Cellulose Nanocrystal-Alginate Hydrogel Beads in  
47  
48 Fixed Bed Columns. *Carbohydr. Polym.* **2016**, *136*, 1194–1202.  
49  
50  
51  
52 (19) Alhamed, Y. A. Adsorption Kinetics and Performance of Packed Bed Adsorber for Phenol  
53  
54 Removal Using Activated Carbon from Dates’ Stones. *J. Hazard. Mater.* **2009**, *170* (2–3),  
55  
56  
57  
58  
59  
60

1  
2  
3  
4  
5  
6  
7  
8  
9  
10  
11  
12  
13  
14  
15  
16  
17  
18  
19  
20  
21  
22  
23  
24  
25  
26  
27  
28  
29  
30  
31  
32  
33  
34  
35  
36  
37  
38  
39  
40  
41  
42  
43  
44  
45  
46  
47  
48  
49  
50  
51  
52  
53  
54  
55  
56  
57  
58  
59  
60

763–770.

(20) Yilmaz, E.; Haupt, K.; Mosbach, K. The Use of Immobilized Templates—A New Approach in Molecular Imprinting. *Angew. Chemie Int. Ed.* **2000**, *39* (12), 2115–2118.

(21) Kong, X.; Gao, R.; He, X.; Chen, L.; Zhang, Y. Synthesis and Characterization of the Core–shell Magnetic Molecularly Imprinted Polymers (Fe<sub>3</sub>O<sub>4</sub>@MIPs) Adsorbents for Effective Extraction and Determination of Sulfonamides in the Poultry Feed. *J. Chromatogr. A* **2012**, *1245*, 8–16.

(22) Roy, D.; Semsarilar, M.; Guthrie, J. T.; Perrier, S. Cellulose Modification by Polymer Grafting: A Review. *Chem. Soc. Rev.* **2009**, *38* (7), 1825–2148.

(23) Moon, R. J.; Martini, A.; Nairn, J.; Simonsen, J.; Youngblood, J. Cellulose Nanomaterials Review: Structure, Properties and Nanocomposites. *Chem. Soc. Rev.* **2011**, *40* (7), 3941–3994.

(24) Del Valle, E. M. M. Cyclodextrins and Their Uses: A Review. *Process Biochem.* **2004**, *39* (9), 1033–1046.

(25) Eftink, M. R.; Andy, M. L.; Bystrom, K.; Perlmutter, H. D.; Kristolt, D. S. Cyclodextrin Inclusion Complexes: Studies of the Variation in the Size of Alicyclic Guests. *J. Am. Chem. SOC* **1989**, *1* (1), 6765–6112.

(26) Sreenivasan, K. Synthesis and Evaluation of a Beta Cyclodextrin-Based Molecularly Imprinted Copolymer. *J. Appl. Polym. Sci.* **1998**, *70* (1), 15–18.

(27) Wang, D.; Liu, L.; Jiang, X.; Yu, J.; Chen, X. Adsorption and Removal of Malachite Green from Aqueous Solution Using Magnetic  $\beta$ -Cyclodextrin-Graphene Oxide Nanocomposites

1  
2  
3 as Adsorbents. *Colloids Surfaces A Physicochem. Eng. Asp.* **2015**, *466*, 166–173.  
4  
5  
6 (28) Chen, L.; Berry, R. M.; Tam, K. C. Synthesis of  $\beta$ -Cyclodextrin-Modified Cellulose  
7 Nanocrystals (CNCs)@Fe<sub>3</sub>O<sub>4</sub>@SiO<sub>2</sub> Superparamagnetic Nanorods. *ACS Sustain. Chem.*  
8 *Eng.* **2014**, *2* (4), 951–958.  
9  
10  
11  
12  
13 (29) Alsbaiee, A.; Smith, B. J.; Xiao, L.; Ling, Y.; Helbling, D. E.; Dichtel, W. R. Rapid  
14 Removal of Organic Micropollutants from Water by a Porous  $\beta$ -Cyclodextrin Polymer.  
15  
16 *Nature* **2016**, *529* (7585), 190–194.  
17  
18  
19  
20  
21 (30) Ling, Y.; Klemes, M. J.; Xiao, L.; Alsbaiee, A.; Dichtel, W. R.; Helbling, D. E.  
22 Benchmarking Micropollutant Removal by Activated Carbon and Porous  $\beta$ -Cyclodextrin  
23 Polymers under Environmentally Relevant Scenarios. *Environ. Sci. Technol.* **2017**, *51* (13),  
24 7590–7598.  
25  
26  
27  
28  
29 (31) Alzate-Sánchez, D. M.; Smith, B. J.; Alsbaiee, A.; Hinestrosa, J. P.; Dichtel, W. R. Cotton  
30 Fabric Functionalized with a  $\beta$ -Cyclodextrin Polymer Captures Organic Pollutants from  
31 Contaminated Air and Water. *Chem. Mater.* **2016**, *28* (22), 8340–8346.  
32  
33  
34  
35  
36  
37  
38  
39 (32) Klemes, M. J.; Ling, Y.; Chiapasco, M.; Alsbaiee, A.; Helbling, D. E.; Dichtel, W. R.  
40 Phenolation of Cyclodextrin Polymers Controls Their Lead and Organic Micropollutant  
41 Adsorption. *Chem. Sci.* **2018**, *9*, 8883–8889.  
42  
43  
44  
45  
46  
47 (33) Kačuráková, M.; Wilson, R. H. Developments in Mid-Infrared FT-IR Spectroscopy of  
48 Selected Carbohydrates. *Carbohydr. Polym.* **2001**, *44* (4), 291–303.  
49  
50  
51  
52  
53 (34) Ghosal, P. S.; Gupta, A. K. Determination of Thermodynamic Parameters from Langmuir  
54 Isotherm Constant-Revisited. *J. Mol. Liq.* **2017**, *225*, 137–146.  
55  
56  
57  
58  
59  
60

1  
2  
3 (35) Liu, Y. New Insights into Pseudo-Second-Order Kinetic Equation for Adsorption. *Colloids*  
4  
5 *Surfaces A Physicochem. Eng. Asp.* **2008**, *320* (1–3), 275–278.  
6  
7  
8 (36) Guiochon, G. Monolithic Columns in High-Performance Liquid Chromatography. *J.*  
9 *Chromatogr. A* **2007**, *1168*, 101–168.  
10  
11  
12  
13  
14  
15  
16  
17  
18  
19  
20  
21  
22  
23  
24  
25  
26  
27  
28  
29  
30  
31  
32  
33  
34  
35  
36  
37  
38  
39  
40  
41  
42  
43  
44  
45  
46  
47  
48  
49  
50  
51  
52  
53  
54  
55  
56  
57  
58  
59  
60

## TOC IMAGE

